1966

Further studies on the lateral-torsional buckling of steel beam-columns, February 1965

P. F. Adams

Y. Fukumoto

T. V. Galambos

Welded Continuous Frames and Their Components

FURTHER STUDIES ON THE LATERAL-TORSIONAL BUCKLING OF STEEL BEAM-COLUMNS

by

Theodore V. Galambos
Peter F. Adams
Yuhshi Fukumoto

Fritz Engineering Laboratory Report No. 205A.36

Welded Continuous Frames and Their Components

FURTHER STUDIES ON THE LATERAL-TORSIONAL BUCKLING OF STEEL BEAM-COLUMNS

by

Theodore V. Galambos

Peter F. Adams

and

Yuhshi Fukumoto

This work has been carried out as part of an investigation sponsored jointly by the Welding Research Council and the Department of the Navy with funds furnished by the following:

American Institute of Steel Construction
American Iron and Steel Institute
Institute of Research, Lehigh University
Column Research Council (Advisory)
Bureau of Ships (Contract No. Nobs 90041)
Bureau of Yards and Docks (Contract No. NBY 53160)
Welding Research Council

Fritz Engineering Laboratory
Lehigh University
Bethlehem, Pennsylvania

February 1965

Fritz Engineering Laboratory Report No. 205A.36

SYNOPSIS

In this report solutions are presented for the inelastic lateral-torsional buckling strength of as-rolled steel wide-flange beam-columns. The beam-columns are subjected to an axial force and to bending moments applied either at one end of the member only or equally to both ends. The reduction in strength as compared with the optimum performance of the member is examined and the influence of the cross-section size, yield stress level, and residual stress level on the lateral-torsional buckling strength is determined. The theoretical solutions are then compared with an empirical reduction formula which is proposed for design purposes. Available test results are compared with the theory as represented by this reduction formula.

TABLE OF CONTENTS

INTRODUCTION

Steel wide-flange members subjected to loads which produce bending about the major axis of the cross section will eventually experience large lateral-torsional deformations which under some conditions may become the primary cause of failure. A complete treatment of this phenomenon is in reality an ultimate strength problem which would involve the determination of the complete load-deformation relationship and include the effect of initial deformations. This, however, is a formidable computational task, and therefore it is customary to idealize the situation and to calculate the loading at which a perfect member may assume both an unbuckled and a buckled deflected shape. The lateral-torsional buckling load of such an ideal member usually provides a reasonable estimate of the ultimate strength of the actual member.

Lateral-torsional buckling may occur when the member is still elastic, or, as is the usual case in steel structures of practical dimensions, when portions of the member have yielded.

This paper will present a discussion of research on the inelastic lateral-torsional buckling strength of as-rolled steel wide-flange beam-columns. This research was performed at Lehigh University as part of a general investigation on the ultimate strength of steel structures. In connection with this work it was realized that no proper understanding of the failure of steel structures can be reached unless the role of the instability phenomena is also well understood. The

major share of this work on inelastic lateral-torsional buckling was performed in the period 1957 to 1963,[1][2] and some parts of it have already been reported.[3][4] One of these reports[3] deals with the lateral buckling of beams, and the other[4] presents the derivation of the equations, outlines of the computational processes, and some of the results for the lateral-torsional buckling strength of beam-columns.

The present paper summarizes the results of the research on inelastic lateral-torsional buckling. First the results of the computations are presented in the form of interaction curves. From these curves the effects of such variables as the cross-sectional size, the residual stress distribution and yield stress level are examined. The theoretical results are next compared to an empirical reduction formula, which is commonly used for the determination of the in-plane strength of beam-columns in the inelastic range. This formula is reviewed in the light of the theoretical work and proposed as a design approximation. Finally the available test results are compared with theory, using the reduction formula as a basis.

LATERAL-TORSIONAL BUCKLING STRENGTH OF BEAM-COLUMNS

The differential equations governing the lateral-torsional buckling of prismatic, singly symmetric members, subjected to centroidal axial forces P and end moments M_o and ρM_o are:(1)(2)(3)(4)

$$B_y u'' + Pu + P_{y_o} \beta - M_o \beta \left[\rho + \frac{z}{L}(1-\rho)\right] = 0 \qquad (1)$$

$$C_w \beta''' - \beta'(C_T + \bar{K}) + P_{y_o} u' - M_o u' \left[\rho + \frac{z}{L}(1-\rho)\right] + M_o \frac{u}{L}(1-\rho) = 0 \qquad (2)$$

The applied moments act in the plane of symmetry, and the origin of the longitudinal coordinate z is chosen such that $M_o \geq \rho M_o$ (Fig. 1 (a)), thus placing ρ within the bounds $-1.0 \leq \rho \leq +1.0$. The variables u and β are, respectively, the lateral deflection of the shear center, S, and the angle of twist of the buckled section about the shear center (Fig. 1 (b)). The primes on u and β in Eqs. (1) and (2) indicate differentiation with respect to z. The coefficients in Eqs. (1) and (2) are defined as follows: (1) B_y is the lateral bending stiffness (EI_y in the elastic range); (2) y_o is the distance between the centroid C and the shear center S in the plane of symmetry (Fig. 1 (b)); (3) C_w is the warping stiffness (EI_w in the elastic range); (4) C_T is the St. Venant torsional stiffness (GK_T in the elastic range); and (5) $\bar{K} = -\int_A \sigma s^2 dA$ where σ is the stress on any cross-sectional element dA (positive in compression) and s is the distance of this element from the shear center. In Fig. 1 (b) the shaded portions shown are those which have yielded under the combined action of the applied forces and residual stresses. It is assumed that

at the instant of buckling the yielded portions of the cross-section are ineffective. Thus the cross-sectional properties are calculated on the basis of the unyielded portions (tangent modulus concept).

In the derivation of the two differential equations it was assumed that P retains its original direction, the member is perfectly straight and uniform, the deflections are small and the cross section does not change its original shape.[1][2][3][4] The smallest value of M_o satisfying both Eqs. (1) and (2) for a given beam-colum subjected to infinitesimal deformations u and β represents the critical loading on the member.

EQUAL END MOMENTS ($\rho = 1.0$)

In the case of equal end moments Eqs.(1) and (2) can be reduced to:

$$B_y u'' + Pu + P_{y_o}\beta - M_o\beta = 0 \tag{3}$$

$$C_w\beta''' - \beta'(C_T + \bar{K}) + P_{y_o} u' - M_o u' = 0 \tag{4}$$

In the elastic range, where the coefficients of these equations are constant, a direct solution is possible.[5][6] In the inelastic range the cross-sectional properties (B_y, C_T, C_w, y_o and $\bar{K}$) depend upon the extent of yielding. Since the bending moment along the length of the beam-column is equal to the applied end moment plus the product of the axial load times the deflection, the extent of yielding, and thus the cross-sectional properties, will vary along the member length. Under these conditions the solution involves not only the solving of two differential equations by finite differences but also a trial and error

procedure.[4]

A considerable simplification can be achieved by assuming the cross-sectional properties to be constant along the length of the member.[1] Under this assumption the buckling strength can be determined directly as:

$$\left[P - \frac{\pi^2 B_y}{L^2}\right]\left[\bar{K} - C_T - \frac{\pi^2 C_w}{L^2}\right] - \left[P_{y_o} + M_o\right]^2 = 0 \qquad (5)$$

Specific solutions based on Eq. (5) are given in Figs. 3, 4 and 5 for wide-flange members having an idealized stress-strain curve and residual stress pattern shown in Fig. 2. The members are of A7 steel. (σ_y = 33 ksi; E = 30,000 ksi; G = 11,500 ksi).

The interaction curves of Figs. 3,4 and 5 relate the applied end moment M_o (non-dimensionalized by M_p, the full plastic moment for P = 0)to the length L (non-dimensionalized by r_y, the minor radius of gyration of the section) for specific constant values of the axial load P (non-dimensionalized by $P_y = A\sigma_y$, the yield load). The curves are for torsionally simply supported end conditions, that is u = β = 0 and u" = β " = 0 at the ends. The ends are thus unable to twist and deflect laterally, but the end section is free to warp. Each curve starts at M_o = 0 at a length where the member would buckle about its weak axis as a pinned-end column, and it is discontinued at L = 25 r_y. For shorter members some of the sssumptions used in developing the curves are no longer valid. At these short lengths full plastification of the section or local buckling would govern the strength.[7]

The information contained in Figs. 3, 4 and 5 pertains to both elastic and inelastic buckling, the two regions being separated by a dashed line. The inelastic portions of the curves were computed on the assumption that yielding along the whole length is uniform, and that the extent of the yielded regions is everywhere governed by the conditions at the ends (that is, P and M_o).[1] Since yielding within the span is more severe than at the ends (because of the increased moment due to the axial load times the deflection), the actual buckling moment is less than that shown. It has been shown[8] that these curves correspond to an upper bound for the critical moment.

A lower bound for the critical moment can be obtained by taking the upper bound value of M_o as the moment at mid-span of the beam-column and determining the corresponding value of the end-moment from column-deflection-curve theory.[9] Fig. 6 diagrammatically shows the significance of the upper and lower bound solution. The actual bending moment diagram, which could be computed by means of the method used in Reference 4 is also shown in this figure.

Fig. 7 shows the magnitude of the error involved in using the curves of Fig. 3, 4, and 5 for the cases investigated. It can be seen that for practical ranges of column length the upper and lower bounds approach one another whereas for more slender columns, (and for columns under higher axial load), the results given by Fig. 3, 4, and 5 are non-conservative and the lower bound should be established.

ONE END MOMENT ($\rho = 0$)

In the case of the member subjected to one end moment Eqs. (1) and (2) (with P = 0) cannot be solved directly, even in the elastic range, and approximate methods must be used to obtain a solution.[10,11] In the inelastic range the variation of the cross-sectional properties along the length of the member must be accounted for[2] and this method of solution has been described in detail in a previous report.[4] This report also contains the derivation of Eqs. (1) and (2) for inelastic buckling and the development of equations, computer programs and charts for the cross-sectional properties (B_y, y_o, C_T, C_w, $\bar{K}$).

The solutions obtained for the 8WF31 member under various axial loads are shown in Fig. 8. These curves consider the variation of yielding along the length of the member (including the effect of the secondary moment)[2][4] and thus they represent an answer which is analytically correct within the framework of the original assumptions. The curves again start at $M_o = 0$ at a length where the member would buckle about its weak axis as a pinned-end column and are discontinued at $L = 25\ r_y$. The boundary between the elastic and inelastic regions is shown as a dashed line.

VARIABLES AFFECTING THE LATERAL-TORSIONAL BUCKLING STRENGTH

The interaction curves presented in Figs. 3,4,5 and 8 represent the basic material from which a number of qualitative and also some quantitative observations concerning the lateral-torsional buckling strength of as-rolled steel wide-flange beam-columns will be made.

Lateral-torsional buckling can affect the load-deformation behavior by reducing the strength and the rotation capacity.[12] The analytical work reported here cannot, by the very nature of the solutions, consider the deformations of beam-colums beyond the start of lateral-torsional buckling. The post-buckling deformation behavior is by far the most important of the two problems, but no feasible method of treating it is as yet available. Thus the remarks in this report will be mainly concerned with the influence of lateral-torsional buckling on the strength of beam-columns.

This effect is illustrated in Fig. 9 where the relationship between M_o and the strong axis slenderness ratio L/r_x of an 8WF31 member subjected to an axial force of $0.3\ P_y$ and equal end moments is examined. The upper curve in this figure corresponds to the ultimate strength where failure is due to inelastic instability in the plane of the applied moments[13], and it represents the optimum performance of this member. The lower curves in Fig. 9 give the strength as governed by elastic and inelastic lateral-torsional buckling for the case of simply supported lateral-torsional end conditions. It is seen that lateral-torsional buckling

is responsible for a considerable reduction in strength. The behavior of the beam-column subjected to one end moment is similar.[4]

1. The Influence of Cross-Sectional Size

The in-plane ultimate strength interaction curves are not sensitive to changes in the cross-sectional size for rolled wide-flange shapes, and one set of curves for any given value of the end moment ratio is sufficient.[13] Thus, the upper curve in Fig. 9 and also in Fig. 10 is valid for any wide-flange section. Unfortunately this is not so for the lateral-torsional buckling strength, as can be seen in Figs. 4 and 5 where, for a constant value of P/P_y, the critical moment is less for the 27WF94 section than for the 14WF142 section. This point is also illustrated in Fig. 10, which compares the lateral-torsional buckling interaction curves for four representative wide-flange shapes with their in-plane interaction curve.

A dimensional analysis was performed to study which of the cross-sectional parameters in Eqs. (1) and (2) had the greatest influence.[1] It was found that for constant values of L/r_y and P/P_y, and the same material, only one non-dimensional ratio was primarily responsible for changes in the critical moment in both the elastic and the inelastic range. This parameter was the ratio $\frac{K_T}{Ad^2}$ (where K_T is the St. Venant torsion constant, A is the area, and d is the depth of the section) and lateral-torsional buckling strength was shown to be proportional to it. The parameter $\frac{K_T}{Ad^2}$ is similar to the torsional constant $T = \frac{GK_T d^2}{4Ar_x^4}$ which had been used by the Cambridge

University group working on the problem of beam columns subjected to bending about both principal axes[14]. It can be seen that the 27WF94 ($\frac{K_T \times 10^6}{Ad^2} = 219$) is a relatively weak section, and the 14WF142 ($\frac{K_T \times 10^6}{Ad^2} = 1580$) is a torsionally strong section.

Values of $\frac{K_T \times 10^6}{Ad^2}$ are tabulated in Table I for many of the shapes listed by the AISC[15]. This table provides a qualitative comparison of the lateral-torsional buckling behavior of all the wide-flange shapes. Shapes which are predominantly used as columns (that is sections for which the depth is approximately the same as the flange width) have $\frac{K_T \times 10^6}{Ad^2}$ ratios usually above 1,000, whereas shapes used as beams fall below this value. Thus fortunately, shapes likely to be subjected to relatively high axial loads have strong lateral-torsional properties.

In addition to the qualitative observations noted above it is possible to arrive at some quantiative conclusions which are quite important from a practical point of view. From Fig. 10 it is seen that for the two 14 in. sections the lateral-torsional buckling curves cross the in-plane curve, and that therefore the strength for shorter lengths is governed by the in-plane ultimate strength. It is significant to note that for the 14WF246 section the reduction due to lateral-torsional buckling is quite small even before the cross-over-point. Thus, it is possible that for many sections of practical lengths no consideration need be given to lateral-torsional buckling.

This problem has been further explored in Reference 1, where an

approximate formula was developed for the limiting length below which the full strength of the section can be developed. As has been noted before, all non-dimensional cross-sectional variables except $\frac{K_T}{Ad^2}$ are approximately constant for constant values of P/P_y and L/r_y even in the inelastic range, and therefore it is possible to construct curves such as those in Fig. 11 where the limiting slenderness ratio is plotted as a function of $\frac{K_T \times 10^6}{Ad^2}$ and P/P_y. These curves are based on a formula and charts given in Reference 1, and they hold approximately true for all wide-flange shapes. The accuracy of the curves can be gaged by the values for the 14WF246 section (round dots) which were obtained from a graphical determination of the intersection points of the lateral-torsional buckling curves of Fig. 4 with the in-plane strength curves. For a given P/P_y the curve in Fig. 11 represents the limiting slenderness ratio at which the ultimate strength solution and the lateral-torsional buckling solution coincide. For larger values of L/r_y lateral-torsional buckling governs, and for smaller values the ultimate strength can be reached. For example if $P/P_y = 0.3$, $\frac{K_T \times 10^6}{Ad^2} = 2500$ and $L/r_y = 80$, the in-plane ultimate strength can be reached.

The significance of the results given in Fig.11 is that (1) for sections having $\frac{K_T \times 10^6}{Ad^2} \leq 1{,}000$, lateral-torsional buckling will always govern, and (2) below $L/r_y = 60$ and for $P/P_y \leq 0.7$ the full capacity of members is achieved for sections having values of $\frac{K_T \times 10^6}{Ad^2}$ above approximately 1500. This includes the majority of the 8, 10, 12 and 14 in. column sections. It should be also noted that the curves in Fig.11 are for laterally and torsionally pinned conditions. In practical cases there will be always some degree of end restraint present,

and so the curves represent a lower bound. Also, these curves are for equal end moments ($\rho = +1.0$), which is again one of the most severe end conditions. Finally, it is possible that the lateral-torsional buckling curve will be very close to the ultimate strength curve even before the cross-over, as in the case of the 14WF246 section (see Fig. 10). Thus the curves given in Fig. 11 would in general be on the conservative side, and it may be safely concluded that for beam-columns having a value of $\frac{K_T \times 10^6}{Ad^2}$ larger than 1,500 no reduction in strength due to inelastic lateral-torsional buckling need be considered. In doubtful cases it is always possible to check Fig. 11, or to perform the calculations with the aid of Reference 1.

2. The Influence of the Yield Stress Level

In the preceeding sections the lateral-torsional buckling strength relationships have been developed for A7 steel. For rolled shapes this steel has a minimum yield stress level of 33 ksi and an average maximum compressive residual stress level of $0.3\sigma_y$ (9.9 ksi) in the flange tips. The typical residual stress distribution for this steel is given in Fig. 2.[16]

It has been tentatively stated that for the common rolling and straightening processes the residual stress distribution does not change significantly with an increase in yield stress.[17] Thus, for A-441 members having a static yield stress of 50 ksi the maximum compressive residual stress is still of the order of the 9.9 ksi which was found to be typical for A7 steel. Although more testing is necessary before this conclusion can be fully substantiated, the comparisons made in this section will be on the basis of a constant value of σ_{RC} = 9.9 ksi and

the typical distribution shown in Fig. 2.

Fig. 12 gives the lateral-torsional buckling strength curves for an 8WF31 section subjected to an axial load $P/P_y = 0.2$ and bent by equal end moments about its strong axis. The curves are terminated on the slenderness ratio (L/r_y) axis at a point corresponding to weak axis Euler buckling. For a constant axial load but for different yield stress levels the termination points can be related as follows:

$$(L/r_y)_{\sigma_y} = (L/r_y)_{33}\sqrt{\frac{33}{\sigma_y}} \qquad (6)$$

From Fig. 12 it can be seen that the influence of the yield stress level on the inelastic portion of the curve is negligible. In the elastic portion of the curves the increase in the yield stress level shifts the elastic lateral-torsional buckling curves to the left. This would mean that for a higher strength member elastic lateral-torsional buckling would occur at a shorter length than for an A7 member. The actual shapes of the column curves are very similar. Fig. 12 compares three yield stress levels (σ_y = 33 ksi; 50 ksi and 100 ksi).

3. <u>The Influence of Residual Stress</u>

Fig. 13 shows the influence of a variation in σ_{RC} on the lateral torsional buckling strength of a typical beam-column. In Fig. 13 the curves are plotted for an 8WF31 member subjected to an axial load of $P/P_y = 0.2$ and bent by equal end-moments about its strong axis.

The yield stress level is maintained at 50 ksi while two values,

$0.2\sigma_y$ and $0.3\sigma_y$, were chosen for the maximum compressive residual stress. These residual stress values are not typical of the measurements made on A441 steel,[17] but the curves of Fig. 13 do serve to illustrate the effect of a change in the residual stress level.

Fig. 13 shows the relationship between the applied end moments and the weak axis slenderness ratio for the two residual stress levels considered. The curves are composed of two definite portions: the elastic portion, for low values of the applied moment, and the inelastic portion as the moment approaches M_{pc} (the full plastic moment reduced by axial load). It should be noted that the $\bar{K}$ term in Eq. (5) is influenced by the residual stress level but the effect in the elastic range is negligible[2] so that at moments below the elastic limit the curves for the two residual stress levels coincide and terminate at a value of L/r_y ($M/M_p = 0$) which corresponds to weak axis buckling.

The primary influence of an increase in the residual stress level is to decrease the value of the applied moment at which the elastic limit is reached. In the inelastic range, the relationships between the applied moment, and the slenderness ratio are almost linear for both the residual stress levels. Since the residual stresses are in equilibrium on any cross-section the two cruves tend toward a value of M_{pc}/M_p at $L/r_y = 0$ regardless of the residual stress level considered.

In summary, an increased residual stress pattern reduces the elastic limit moment of the member and thus causes a reduction in strength in the inelastic range.

COMPARISON WITH A DESIGN APPROXIMATION

The computations employed here to determine the lateral-torsional buckling strength of beam-columns are too tedious for design office use. Methods must be found which will provide safe approximations to the theoretical strength with an economical amount of effort.

The method that is proposed to account for the yielding of the member is similar to that suggested by the Column Research Council for the determination of the critical load of an axially loaded column containing residual stresses.[18] In this procedure the relationship between the critical load and slenderness ratio is first computed by assuming the member to be elastic:

$$\frac{P_e}{P_y} = \frac{\sigma_e}{\sigma_y} = \pi^2 \frac{E}{\sigma_y} \frac{1}{(KL/r)^2} \qquad (7)$$

In Eq. (7) P_e is the Euler buckling load, P_y is the yield load ($A \cdot \sigma_y$) and σ_e and σ_y the corresponding stresses. The non-dimensional effective length of the column is given by KL/r where K is the effective length factor, L is the length of the column, and r is the radius of gyration in the direction of buckling.[18]

This relationship is valid if the load is below that which causes yielding of the material at any point. For loads above this value, the yielded portions of the cross-section are ineffective in resisting the bending that accompanies buckling thus the column curve deviates from the Euler curve and the critical load approaches the yield load as the slenderness ratio approaches zero.

To provide a transition curve for the inelastic region a parabolic curve is used:

$$\frac{\sigma_c}{\sigma_y} = 1 - 0.25\frac{\sigma_y}{\sigma_e} \tag{8}$$

Where σ_c is now the critical stress in the inelastic range. Eq. (8) is used if $\sigma_e > 0.5\sigma_y$ (implying a residual stress level of $0.5\sigma_y$). This procedure has also been used to approximate the lateral-torsional buckling strength of beams subjected to uniform moment[3] and will be used for beam-columns in this report.

The elastic solution for beam-columns subjected to equal end moments is given by Eq. (5). Substituting the elastic values for the coefficients ($B_y = EI_y$, $\bar{K} = \frac{I_x + I_y}{A}$, $C_T = GK_T$, $C_w = EI_w$) and noting that for doubly summetric sections $y_o = 0$, Eq.(5) may be written as

$$\frac{M_o}{M_p} = \sqrt{\frac{(I_x + I_y)A}{Z^2}\left[\frac{P_Y}{P_y} - \frac{P}{P_y}\right]\left[\frac{P_T}{P_y} - \frac{P}{P_y}\right]} \tag{9}$$

In Eq. (9) Z represents the plastic modulus of the cross section, P_Y/P_y and P_T/P_y are nondimensionalized loads given by

$$\frac{P_Y}{P_y} = \frac{\pi^2 E}{\sigma_y(L/r_y)^2} \tag{10}$$

$$\frac{P_T}{P_y} = \frac{GK_T}{\sigma_y(I_x + I_y)}\left[1 + \frac{\pi^2 EA(d-t)^2}{4GK_T(L/r_y)^2}\right] \tag{11}$$

For a given beam-column the maximum elastic stress, σ_e, is given by[5]

$$\frac{\sigma_e}{\sigma_y} = \frac{P}{P_y} + \frac{M_o}{M_p} \frac{f}{\cos.\left[\frac{1}{2}\frac{L}{r_x}\sqrt{\frac{P}{P_y}\frac{\sigma_y}{E}}\right]} \tag{12}$$

where f is the shape factor ($f = Zd/2I_x$)

Following the previous procedure for axially loaded columns, if $\sigma_e/\sigma_y \leq 0.5$ the value of M_o as obtained from Eq. (9) is assumed to be correct. If $\sigma_e/\sigma_y > 0.5$, the adjusted critical stress is first calculated from Eq. (8), then the critical value of the applied end moment is determined from

$$\frac{M_o}{M_p} = \frac{\cos.\left[\frac{1}{2}\frac{L}{r_x}\sqrt{\frac{P}{P_y}\frac{\sigma_y}{E}}\right]}{f}\left[\frac{\sigma_c}{\sigma_y} - \frac{P}{P_y}\right] \tag{13}$$

The above procedure was used to obtain the relationship between slenderness ratio and applied end moment for the 8WF31 and 27WF94 sections. These relationships are shown as the dashed curves in Fig. 14 and 15. In these figures, the solid lines represent the theoretical solutions. Comparisons are made for P/P_y values of 0.3, 0.5 and 0.7.

Under low applied moments, the member remains elastic and the approximate solution coincides with that obtained from theory. The apparent discrepancies near the knee of the curves are due to the neglect of the secondary moments (Figs. 3, 4, and 5) in the theoretical solution. In view of this fact, it appears that in these areas the C.R.C. reduction formula will be closer to the actual situation than

the theoretical solution.

For the 8WF31 section ($\frac{K_T \times 10^6}{Ad^2} = 925$) Fig. 14 shows that the C.R.C. reduction formula provides a good approximation to the theroetical soltuion. It should be noted that for high values of axial load the C.R.C. solution is slightly on the non-conservative side, but in general it may be used with confidence.

The situation is not as good for the torsionally weak 27WF94 section ($\frac{K_T \times 10^6}{Ad^2} = 219$) as shown by Fig. 15. In the inelastic range the C.R.C. reduction formula overestimates the strength of the member. For low and average values of axial load ($P/P_y \leq 0.5$) the error is less than 20%. However, care must be taken in considering torsionally weak members subjected to high axial loads.

For beam-columns subjected to one end moment only an approximate elastic solution must be used as the equations (Eqs. (1) and (2) with $\rho = 0$) cannot be solved exactly. For this case an energy method[10,11] was used to obtain the critical elastic end moments for a given member and axial load.

Once the value of the end moment is known the maximum bending moment (considering secondary effects) can be calculated and the maximum elastic stress, σ_e, determined. If $\sigma_e/\sigma_y \leq 0.5$ the critical end moment is that value obtained from the energy solution. If $\sigma_e/\sigma_y > 0.5$ the reduced critical stress is found from Eq. (8) and the corresponding critical end moment value is determined from a consideration

of the contributions due to axial load and secondary moment.

The dashed curves in Fig. 16 were obtained by the above procedure. The solid curves represent the theoretical solutions for an 8WF31 beam column subjected to one end moment only.

The agreement between the theoretical solutions and the approximate curves is satisfactory although for low slenderness ratios the approximate values are somewhat conservative. The agreement could be improved by choosing a different reduction curve to replace Eq. (8). It appears, however, that having a simple, uniform reduction procedure outweighs any advantage that could be gained in this way.

COMPARISON WITH TEST RESULTS

The comparison of lateral-torsional buckling theory with test results is a painful and unrewarding task. The calculation of the theoretical bifurcation load of various test columns, each having associated with it a particular cross-sectional shape, yield stress level and loading condition, is clearly impossible. In addition to computational difficulties, experimental discrepancies are inevitable: the yield stress level is usually not adjusted to include the influence of strain rate and the loading and restraint conditions are not clearly defined. Finally, as failure of the member is the result of a combination of in and out-of-plane effects, the separation of these factors to determine the experimental bifurcation load is not possible.

However, on a statistical basis the reported experimental results should agree with a rational theory based on an initially perfect member. To avoid the computational difficulties, but to give some basis for comparison, the CRC reduction method, described in the previous section, has been used to estimate for various beam-columns the moment at which bifurcation occurred.

Many of the tests reported were performed under a constant eccentricity ratio, ec/r_x^2, where e is the eccentriciy of the load and c is the half depth of the member. In these cases the maximum moment is obtained from

$$\frac{M}{M_p} = \frac{ec}{r_x^2} \cdot \frac{P}{P_y} \cdot \frac{1}{f} \qquad (14)$$

Sixty tests were selected for comparison with the solution for a beam-column subjected to equal end-moments. These tests were selected from various programs performed at the University of Liege[19], the University of Wisconsin[20] and Lehigh University[16][21][22][23]. The tests used for comparison were those for which failure was due to lateral-torsional buckling. For the sixty tests the ratio of the experimental moment divided by the theoretical bifurcation moment as given by the C.R.C. reduction formula was calculated. The statistical mean value was 1.16 with a standard deviation of 0.21. The frequency histogram for these results is given as Fig. 17.

For comparison with the C.R.C. solution for beam-columns subjected to one end-moment, eighteen tests were selected.[18][23] For these tests the reported failure mode was lateral-torsional-buckling. The ratio of the experimental moment to that given by the C.R.C. formula was again calculated. The statistical mean was exactly 1.00 with a standard deviation of 0.33. The freqency histogram is shown in Fig. 18.

SUMMARY AND CONCLUSIONS

In this report solutions for the lateral-torsional buckling strength of specific wide-flange beam-columns have been presented. These solutions have been examined and the difference in strength from that predicted by in-plane failure theory has been depicted. In addition the influence of cross-section size, yield stress level and residual stress level has been evaluated. Finally the solutions have been compared on a statistical basis with test results and an approximate design procedure has been proposed.

A previous report[4] has provided the derivation of the basic differential equations as well as the method of solution for beam-columns subjected to one end moment. The solution for the veam-column subjected to equal end moments has also been previously reported.[1]

The work of the present report may be summarized as follows:

1. Solutions have been presented for beam-columns subjected to equal end moments or one end moment. These solutions are valid for A7 steel (σ_y = 33 ksi; E = 30,000 ksi; G = 11,500 ksi;) which has a maximum compressive residual stress of $0.3\sigma_y$. The solutions are presented as the curves of Figs. 3,4,5, and 8. It may be shown (Fig. 9) that lateral-torsional buckling in some cases significantly reduces the beam-column strength from that predicted by the in-plane bending theory.

2. Unlike the case of in-plane failure, the lateral-torsional buckling strength depends to a great extent on the shape of the cross-section. This strength is related to the torsional properties of the cross section

and is found to be proportional to K_T/Ad^2. Values of this parameter are given in Table I for many of the shapes in common use. It has been shown that for shapes having $\frac{K_T \times 10^6}{Ad^2} \leq 1{,}000$ the lateral-torsional buckling strength will be less than the in-plane strength and that for $\frac{K_T \times 10^6}{Ad^2} \geq 1{,}500$ the full in-plane capacity of the member may be achieved.

3. The influence of a change in the yield stress level has been investigated. This was accomplished while holding the maximum compressive residual stress at 9.9 ksi. It was found that the influence of this change was negligible in the inelastic range, but for elastic lateral-torsional buckling an increase in yield stress shifted the elastic curve to the left and thus reduced the usable range of slenderness ratios. This is shown in Fig. 12.

4. The influence of a change in residual stress level was investigated. This was performed for a constant value of σ_y = 50 ksi and two values of the maximum compressive residual stress of $0.2\sigma_y$ and $0.3\sigma_y$. An increase in residual stress did not significantly influence the elastic lateral torsional buckling curve but did reduce the inelastic strength. This reduction was directly proportional to the slenderness ratio and is shown in Fig. 13.

5. The theoretical solutions were compared with an empirical reduction formula as suggested by the C.R.C. For beam-columns subjected to equal end moments the agreement was satisfactory. For beam-columns subjected to one end moment the agreement was again satisfactory but slightly conservative for very stocky columns. These comparisons are given in Figs. 14, 15, and 16.

6. The theoretical solutions were compared statistically with available test results. The uncertainty involved in these results justified comparison on an approximate basis. For sixty experiments performed on beam-columns subjected to equal end moments the mean value of the ratio of experimental moment to that given by the C.R.C. reduction formula was 1.16. The standard deviation was 0.21. For beam-columns subjected to one end moment the statistical mean of the ratio was exactly 1.00 with a standard deviation of 0.33. Eighteen tests were used in this latter comparison. The frequency histograms for these results are shown in Figs. 17 and 18.

ACKNOWLEDGEMENTS

This study is part of a general investigation "Welded Continuous Frames and Their Components" currently being carried out at Fritz Engineering Laboratory, Department of Civil Engineering. Professor W. J. Eney is Head of the Civil Engineering Department and Dr. L. S. Beedle is Director of the Laboratory. The investigation is sponsored jointly by the Welding Research Council, and the Department of the Navy, with funds furnished by the American Institute of Steel Construction, the American Iron and Steel Institute, Lehigh University Institute of Research, the Bureau of Ships and the Bureau of Yards and Docks. The Column Research Council acts in an advisory capacity.

NOMENCLATURE

B_y lateral bending stiffness (EI_y in the elastic range)

u lateral deflection of shear center. Primed values denote differentiation with respect to z.

P axial load

β angle of twist of section about Shear center

y_o distance between centroid and shear center in the plane of symmetry

M_o applied end moment

ρ end moment ratio $-1.0 \leq \rho \leq 1.0$

z distance on longitidinal axis

L length of beam

C_W warping stiffness (EI_W in elastic range)

C_T St. Venants torsional stiffness (GK_T in elastic range)

$\bar{K}$ $= -\int_A \sigma s^2 dA$ where σ is the stress on any cross-sectional element dA (positive in compression) and s is the distance of this element from the shear center

σ_y yield stress level. Taken at zero strain rate

E modulus of elasticity

G	modulus of rigidity
r_y	minor radius of gyration
r_x	major radius of gyration
P_y	$\sigma_y \cdot A$ where A is the cross-section area
M_p	full plastic moment
M_{pc}	full plastic moment reduced by axial load
K_T	St. Venant torsion constant
d	depth of section
σ_{RC}	maximum compressive residual stress.
f	shape factor = $Zd/2I_x$

SECTION	$\frac{K_T \times 10^6}{Ad^2}$	r_x/r_y	SECTION	$\frac{K_T \times 10^6}{Ad^2}$	r_x/r_y	SECTION	$\frac{K_T \times 10^6}{Ad^2}$	r_x/r_y
36WF300	578	4.06	21WF55	190	5.09	12WF190	4329	1.79
36WF230	354	4.14	18WF114	867	2.82	12WF106	1785	1.76
36WF194	312	5.85	18WF96	646	2.84	12WF65	786	1.75
36WF135	150	6.15	18WF85	695	3.78	12WF58	842	2.10
33WF240	496	3.94	18WF64	426	3.87	12WF53	709	2.11
33WF200	356	4.00	18WF60	408	4.58	12WF50	830	2.64
33WF152	263	5.64	18WF45	227	4.71	12WF40	578	2.62
33WF118	152	5.87	16WF96	899	2.56	12WF36	568	3.43
30WF210	539	3.74	16WF88	769	2.57	12WF27	343	3.51
30WF172	376	3.78	16WF78	833	3.46	10WF112	3600	1.75
30WF132	291	5.58	16WF58	497	3.52	10WF72	1809	1.72
30WF99	158	5.85	16WF50	418	4.34	10WF49	966	1.71
27WF177	555	3.60	16WF36	222	4.47	10WF45	1130	2.16
27WF145	394	3.64	14WF426	7757	1.67	10WF33	639	2.16
27WF114	256	5.23	14WF320	5147	1.59	10WF29	696	3.20
27WF94	219	5.32	14WF246	3712	1.62	10WF21	329	3.31
27WF84	170	5.42	14WF142	1580	1.59	8WF67	3221	1.75
24WF160	621	3.23	14WF136	1570	1.68	8WF40	1413	1.73
24WF130	421	3.27	14WF111	1124	1.67	8WF31	925	1.73
24WF120	423	3.79	14WF87	742	1.66	8WF28	1010	2.13
24WF100	309	3.83	14WF84	901	2.03	8WF24	789	2.12
24WF94	342	5.12	14WF78	766	2.03	8WF20	590	2.86
24WF68	117	5.32	14WF74	895	2.46	8WF17	500	2.91
21WF142	793	2.97	14WF61	640	2.44	6WF25	1598	1.78
21WF112	521	3.01	14WF53	630	3.07	6WF20	1108	1.77
21WF96	544	4.36	14WF43	447	3.08	6WF15.5	709	1.77
21WF82	412	4.42	14WF38	386	3.87	5WF18.5	2100	1.69
21WF73	334	4.90	14WF30	242	3.99	4WF13	2358	1.74

TABLE 1 Torsional Properties

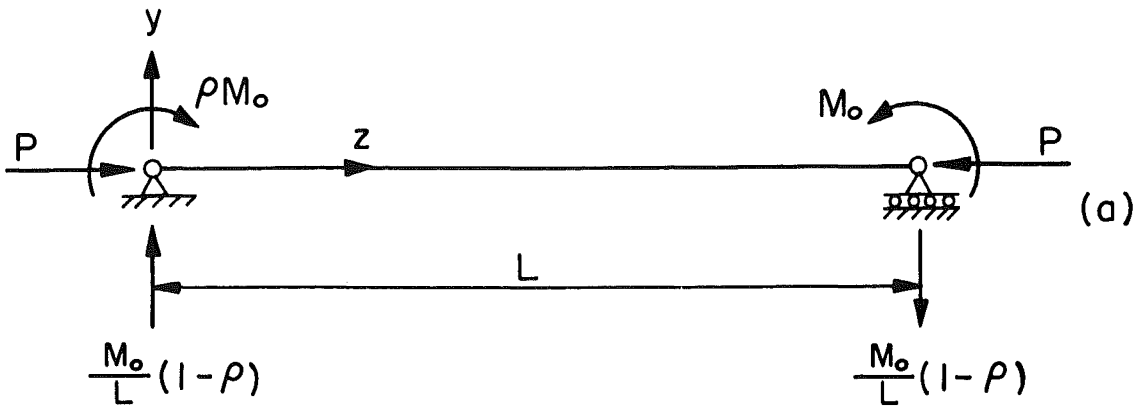

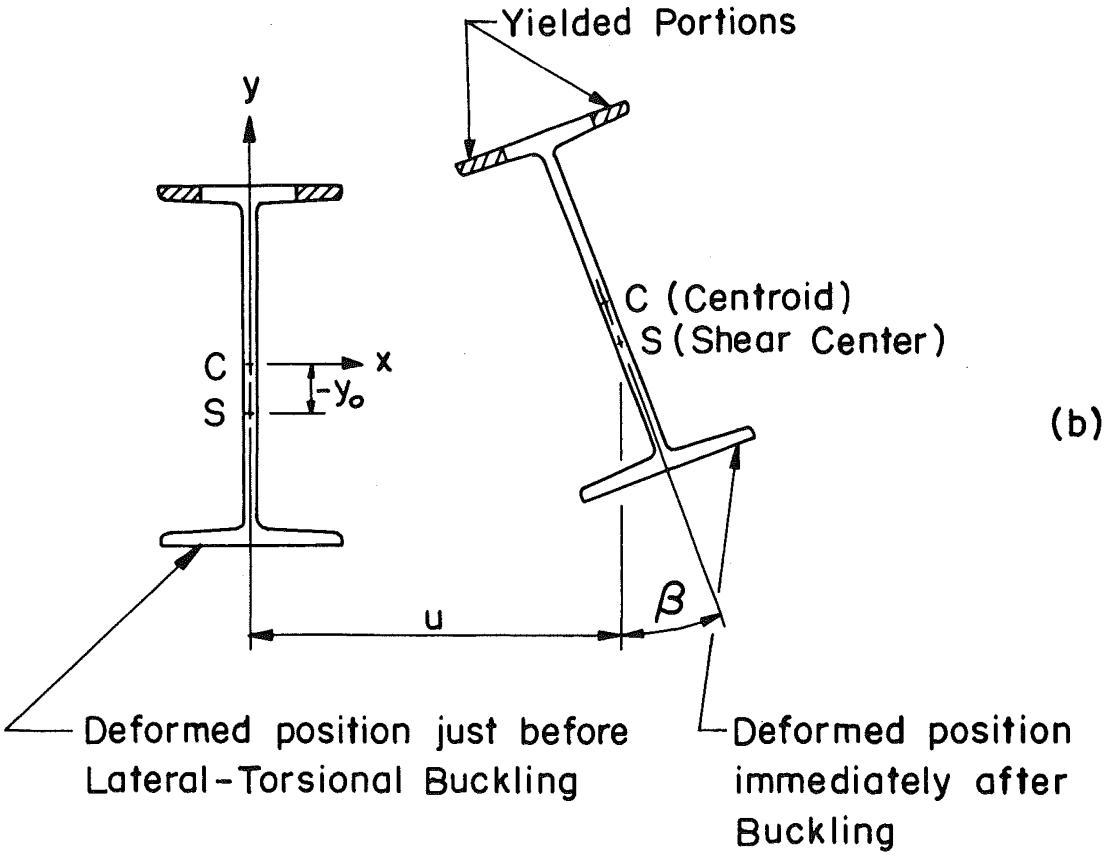

Fig. 1 Loading, Geometry and Deformed Position of the Member

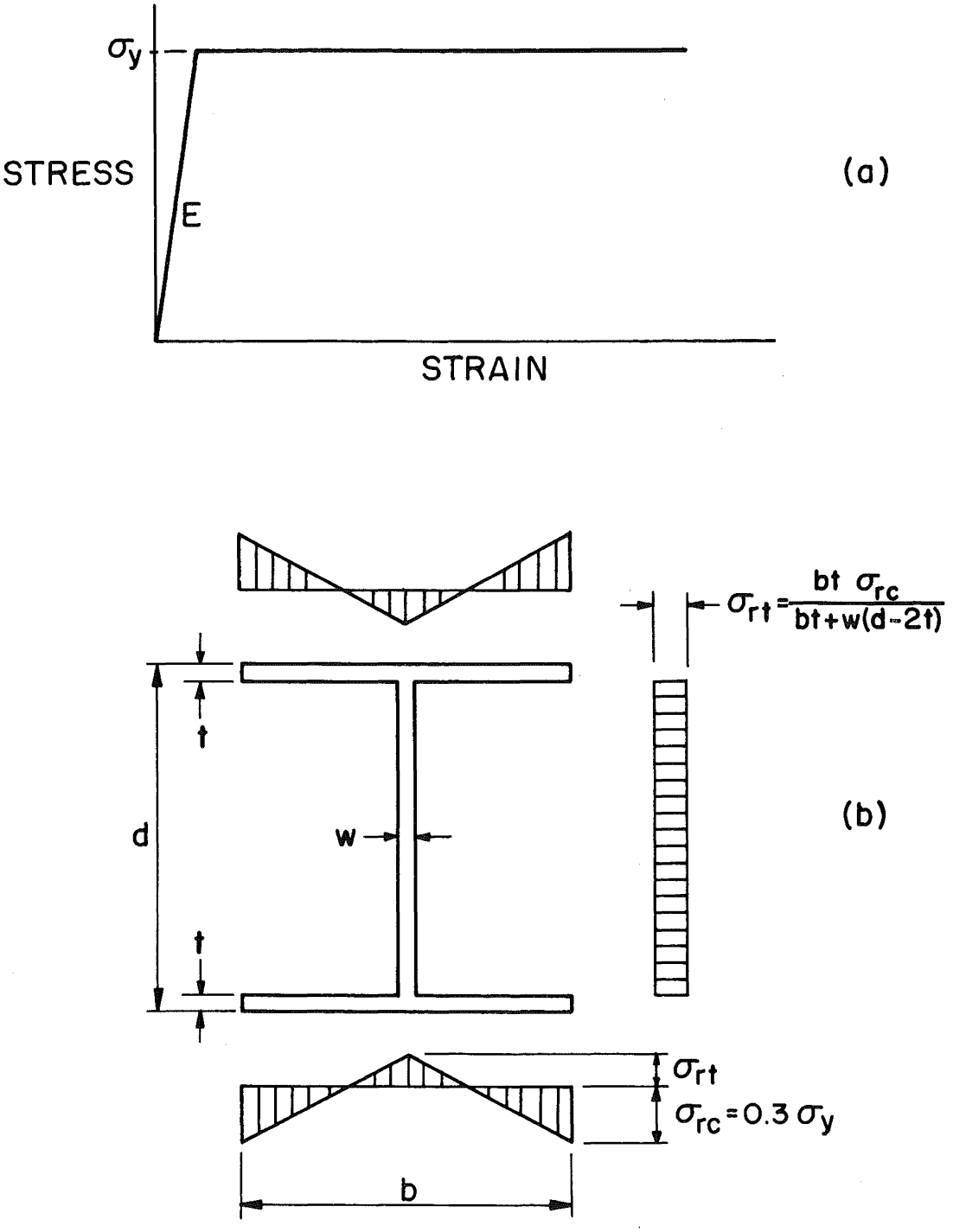

σ_{rc} : Maximum Compressive Residual Stress
σ_{rt} : Maximum Tensile Residual Stress

Fig. 2 Stress-Strain Diagram and Residual Stress Distribution

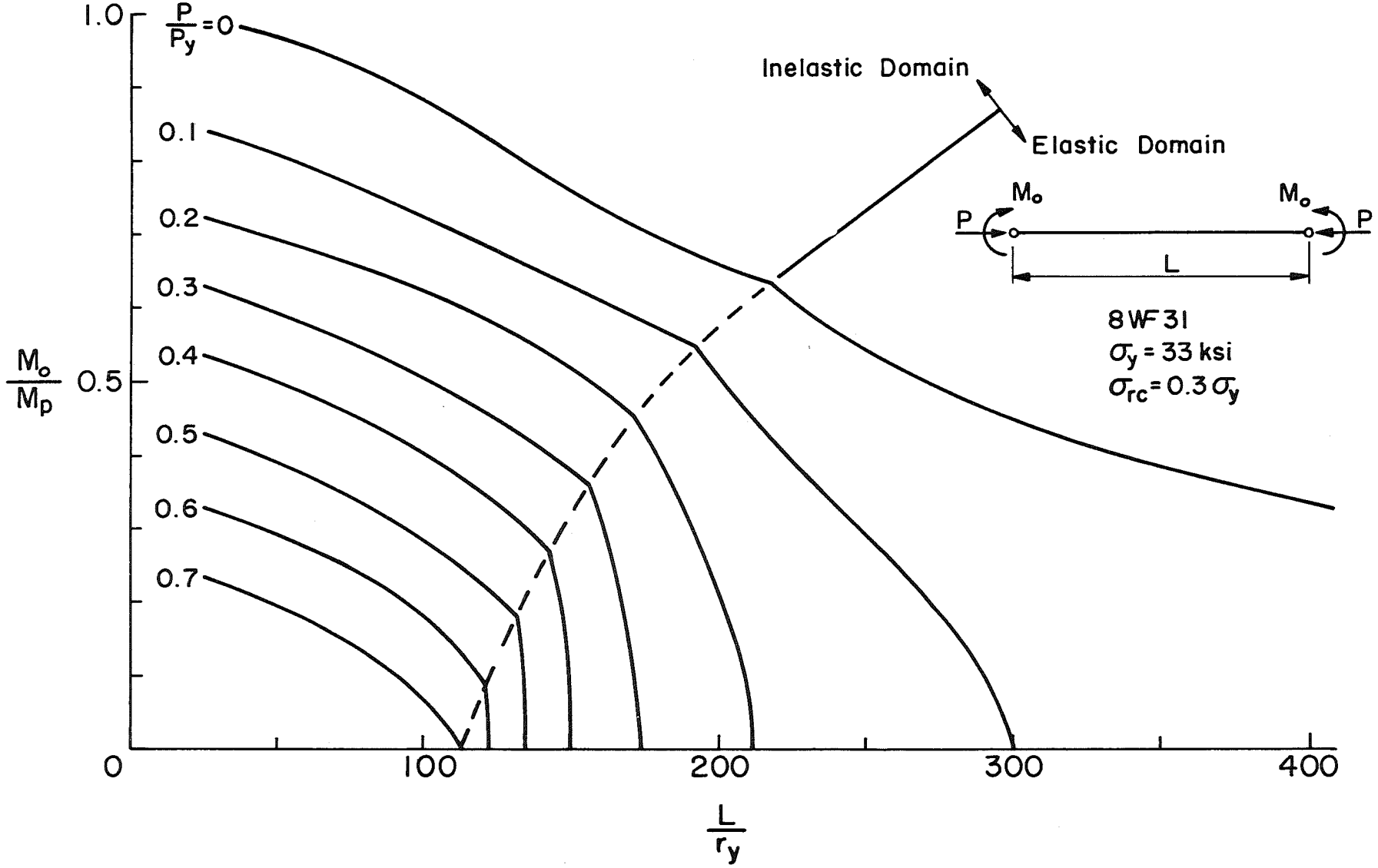

Fig. 3 Interaction Curves for ρ = +1.0 (Uniform Yielding) 8WF31

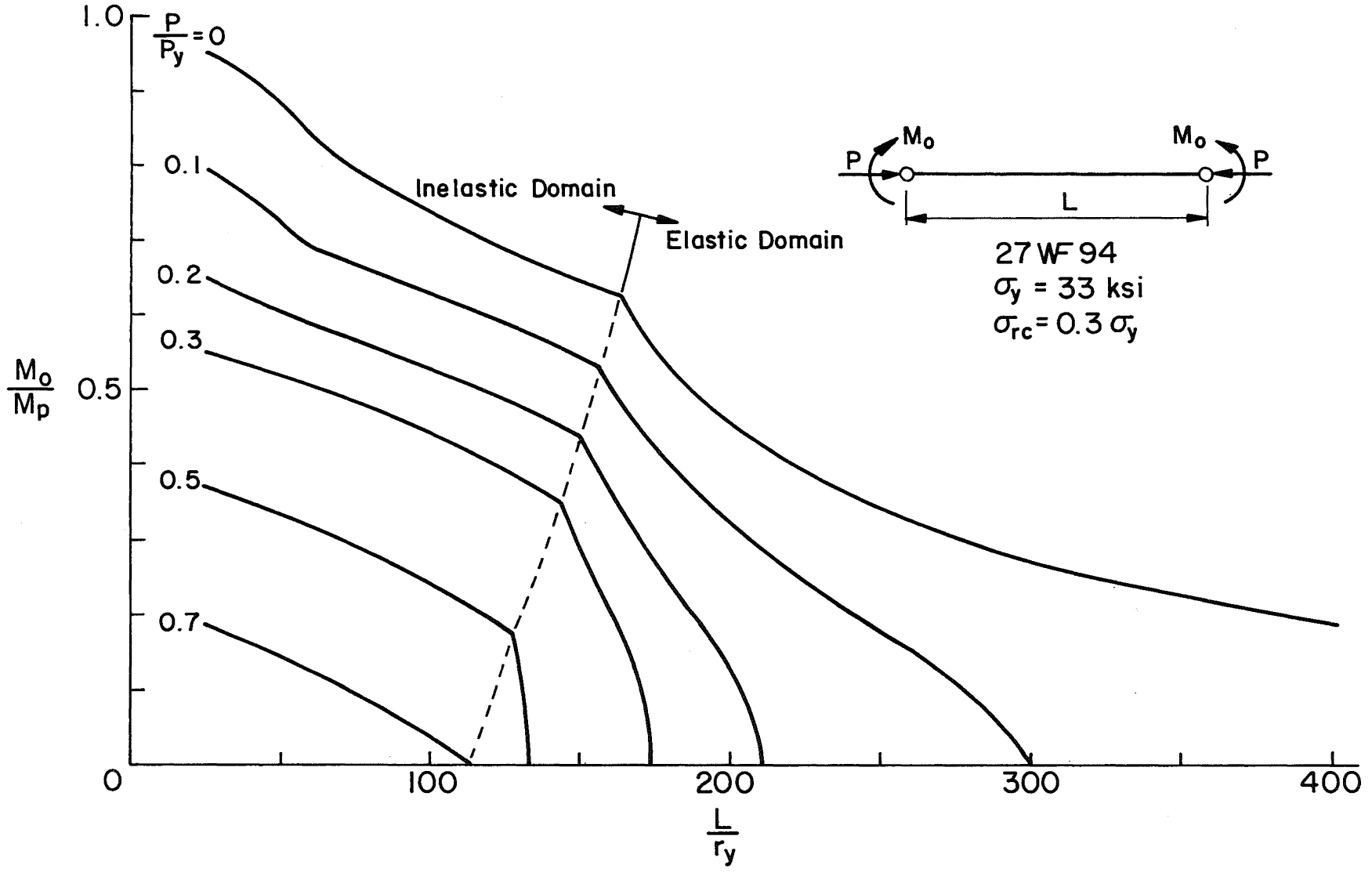

Fig. 4 Interaction Curves for $\rho = +1.0$ (Uniform Yielding) 27WF94

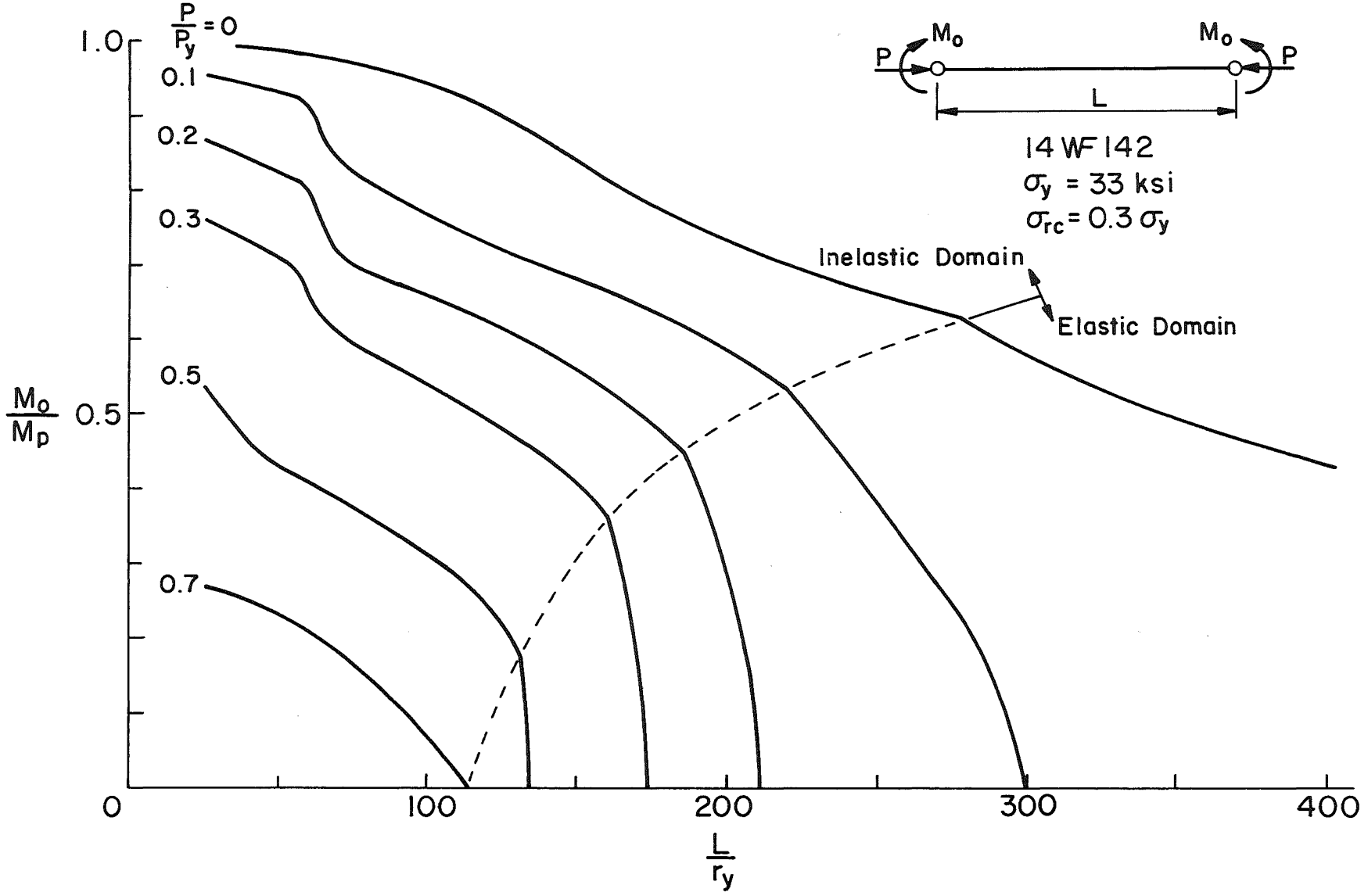

Fig. 5 Interaction Curves for $\rho = +1.0$ (Uniform Yielding) 14WF142

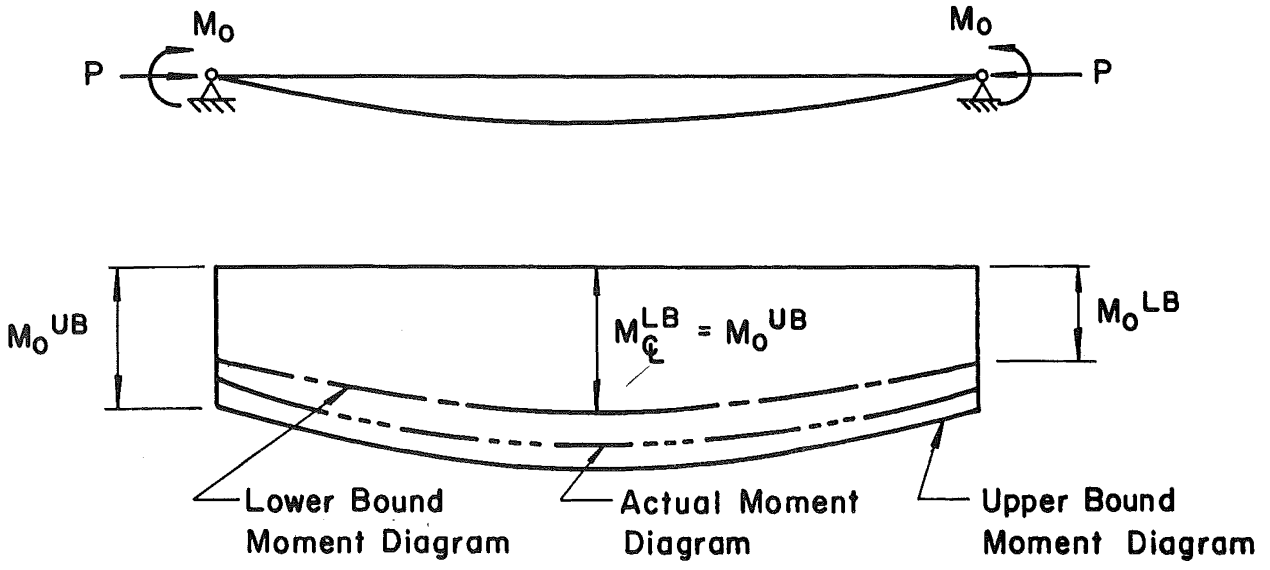

Fig. 6 Upper and Lower Bounds of Lateral-Torsional Buckling Strength

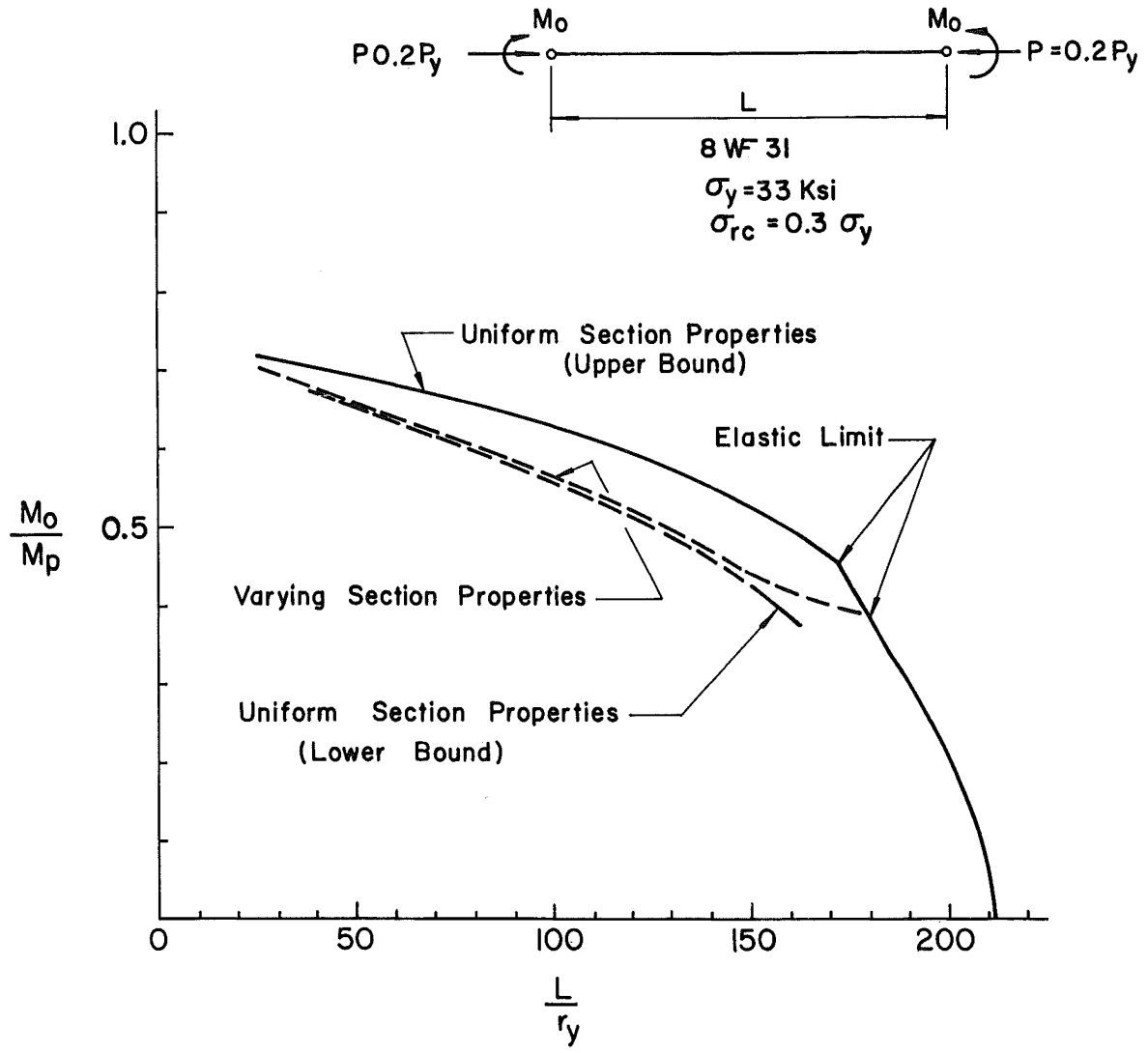

Fig. 7 The Effect of Secondary Moments on Lateral-Torsional Buckling

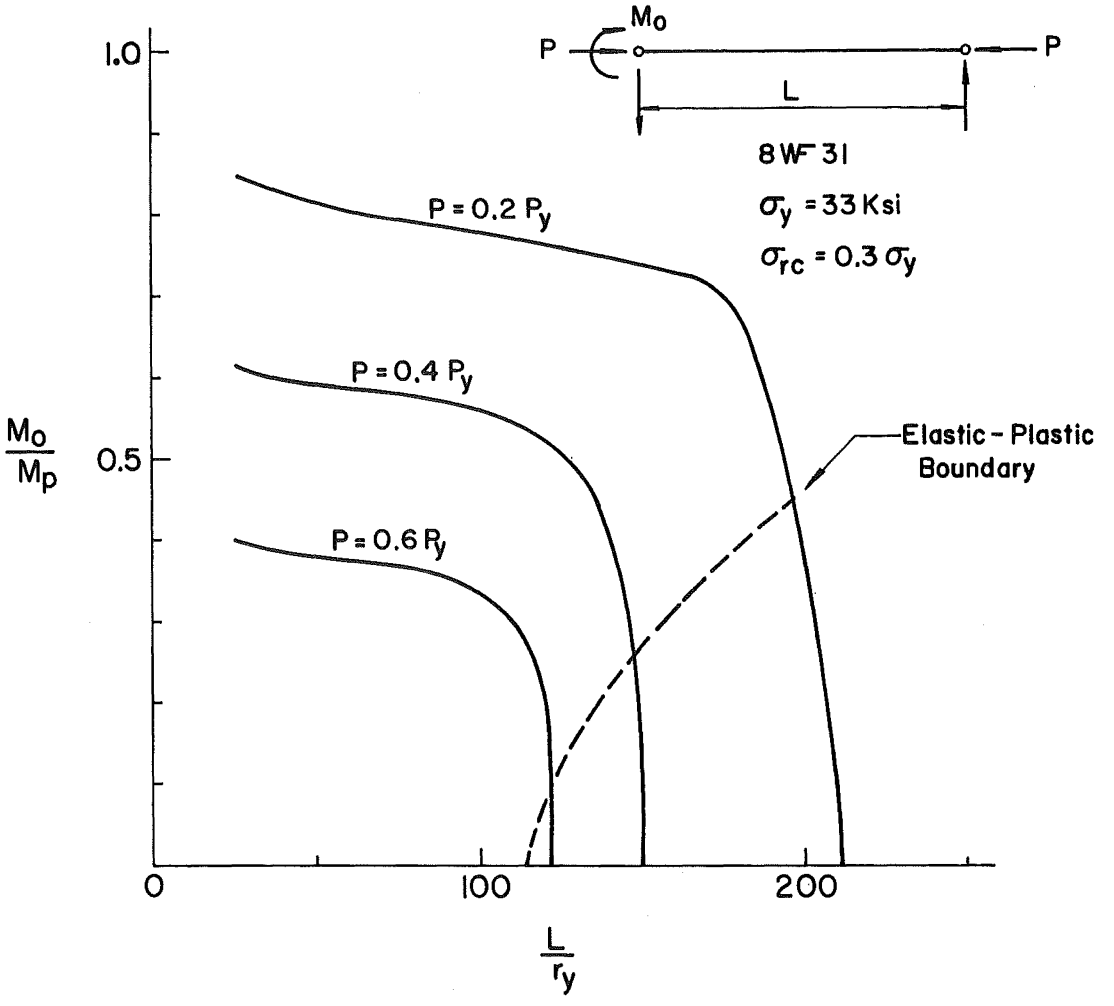

Fig. 8 Interation Curves for $\rho = 0$ 8WF31

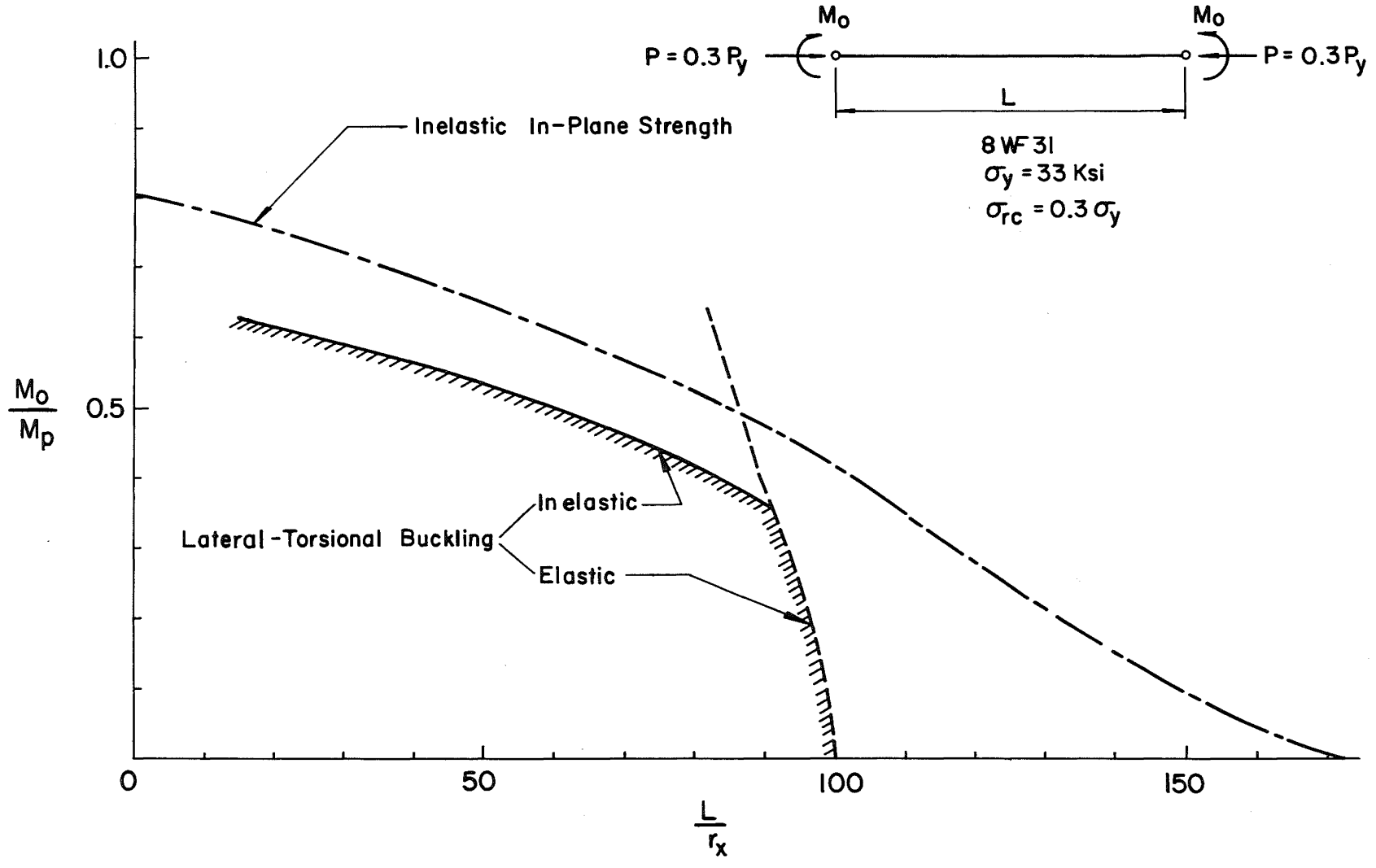

Fig. 9 The Effect of Lateral-Torsional Buckling on the Strength of Beam-Columns

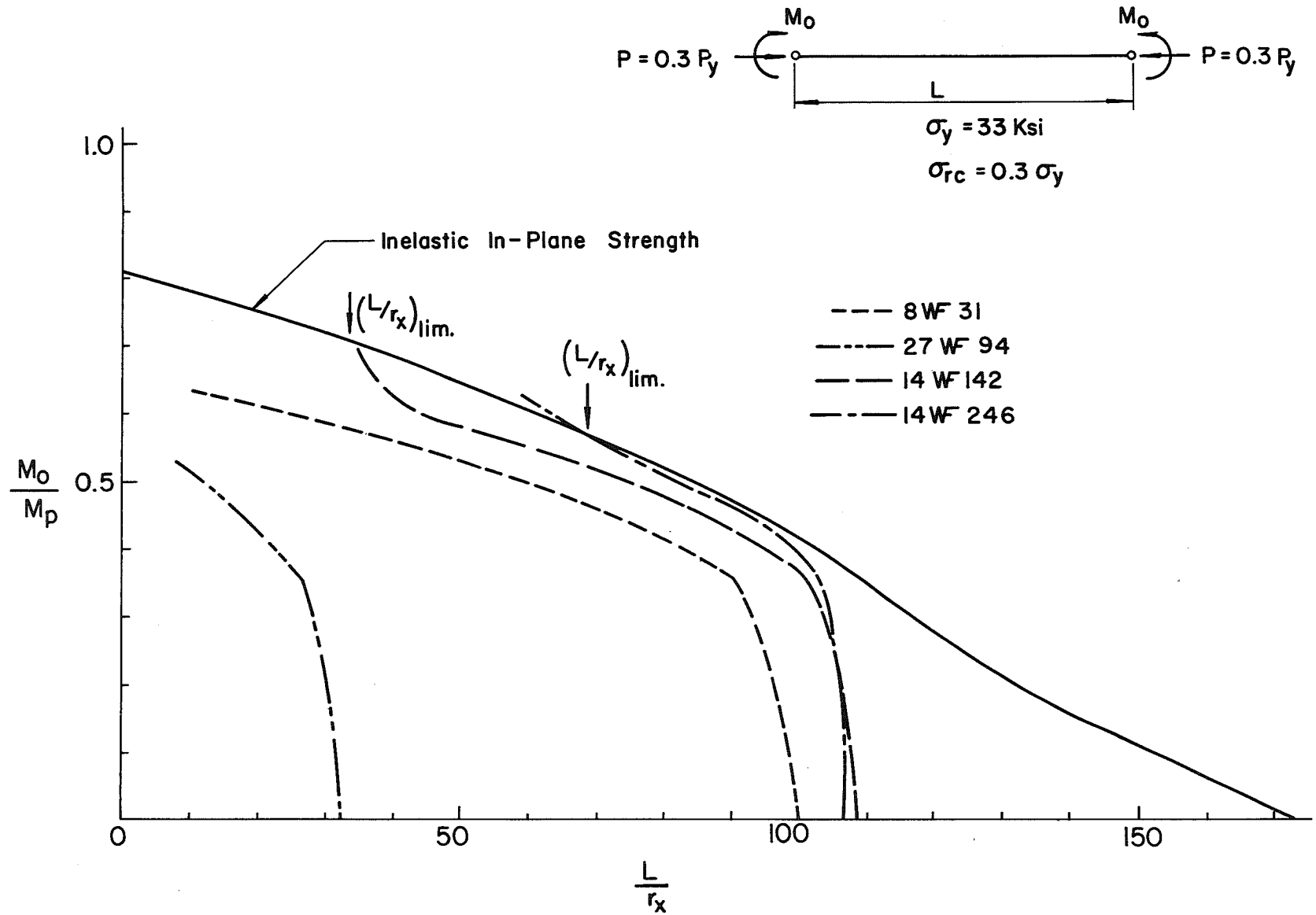

Fig. 10 The Effect of Cross-Sectional Shape on Lateral-Torsional Buckling

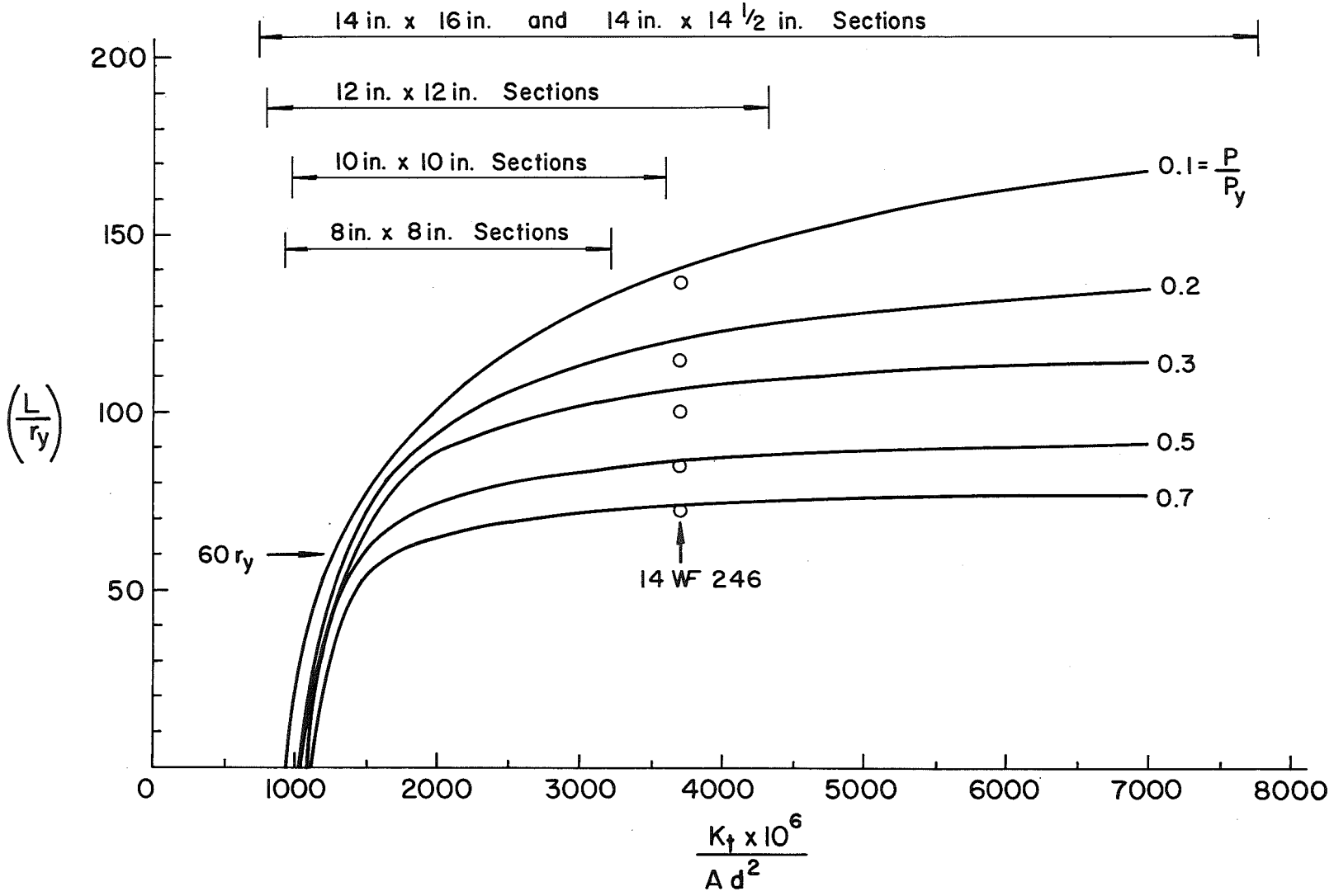

Fig. 11 Limits for Exclusion of Lateral-Torsional Buckling

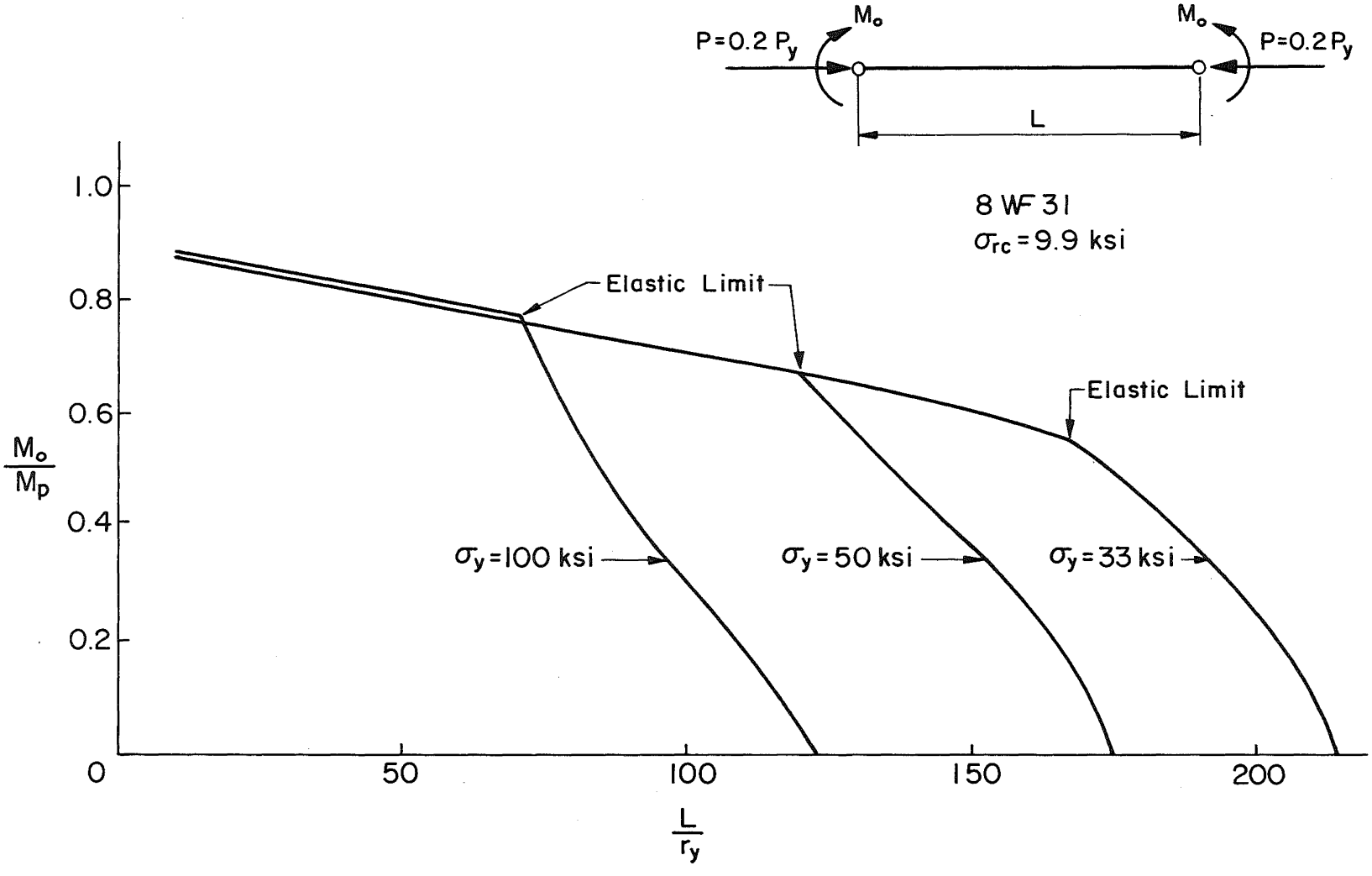

Fig. 12 Effect of Yield Stress Level on Lateral-Torsional Buckling Strength

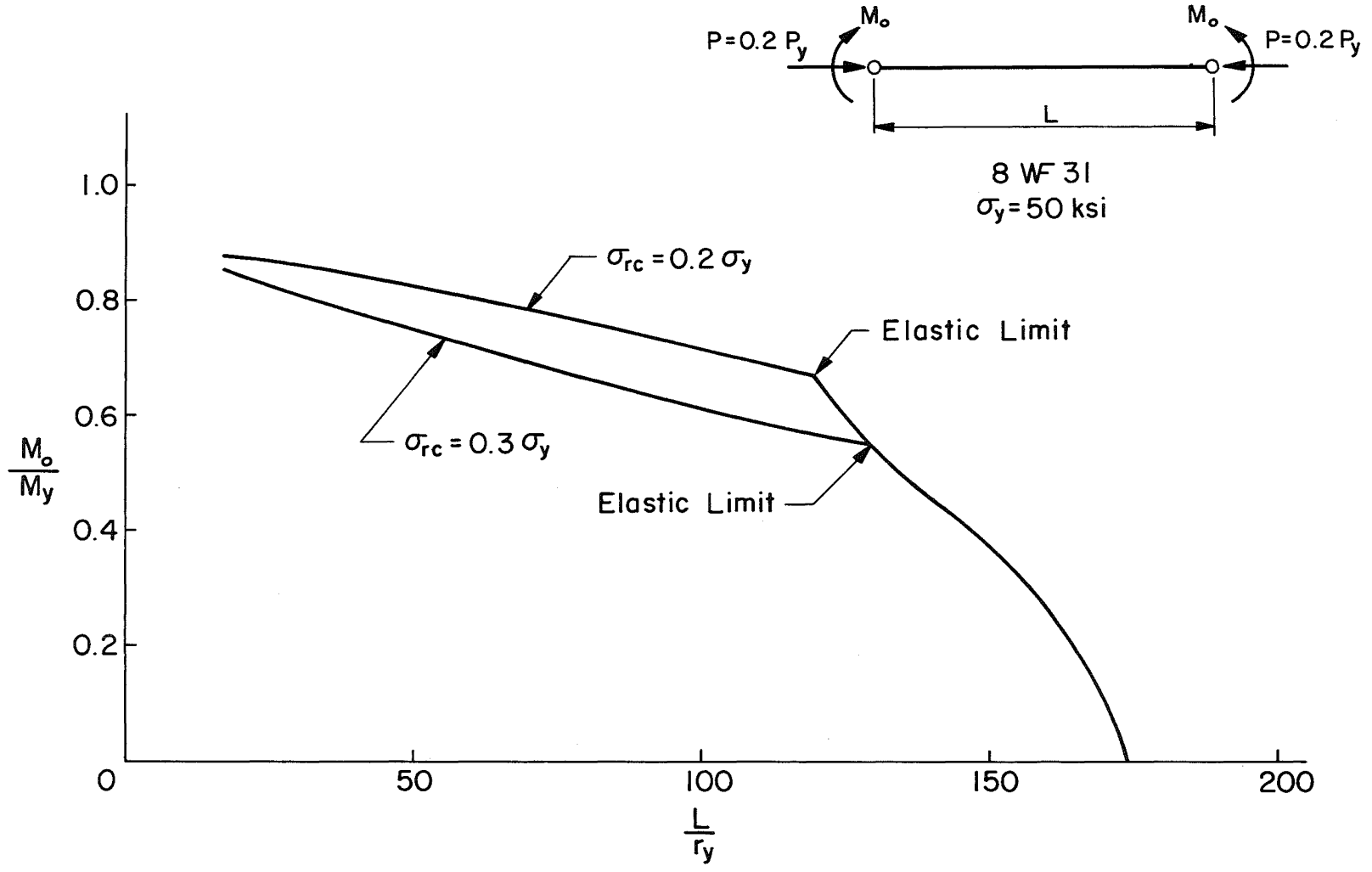

Fig. 13 Effect of Residual Stress Level on Lateral-Torsional Buckling Strength

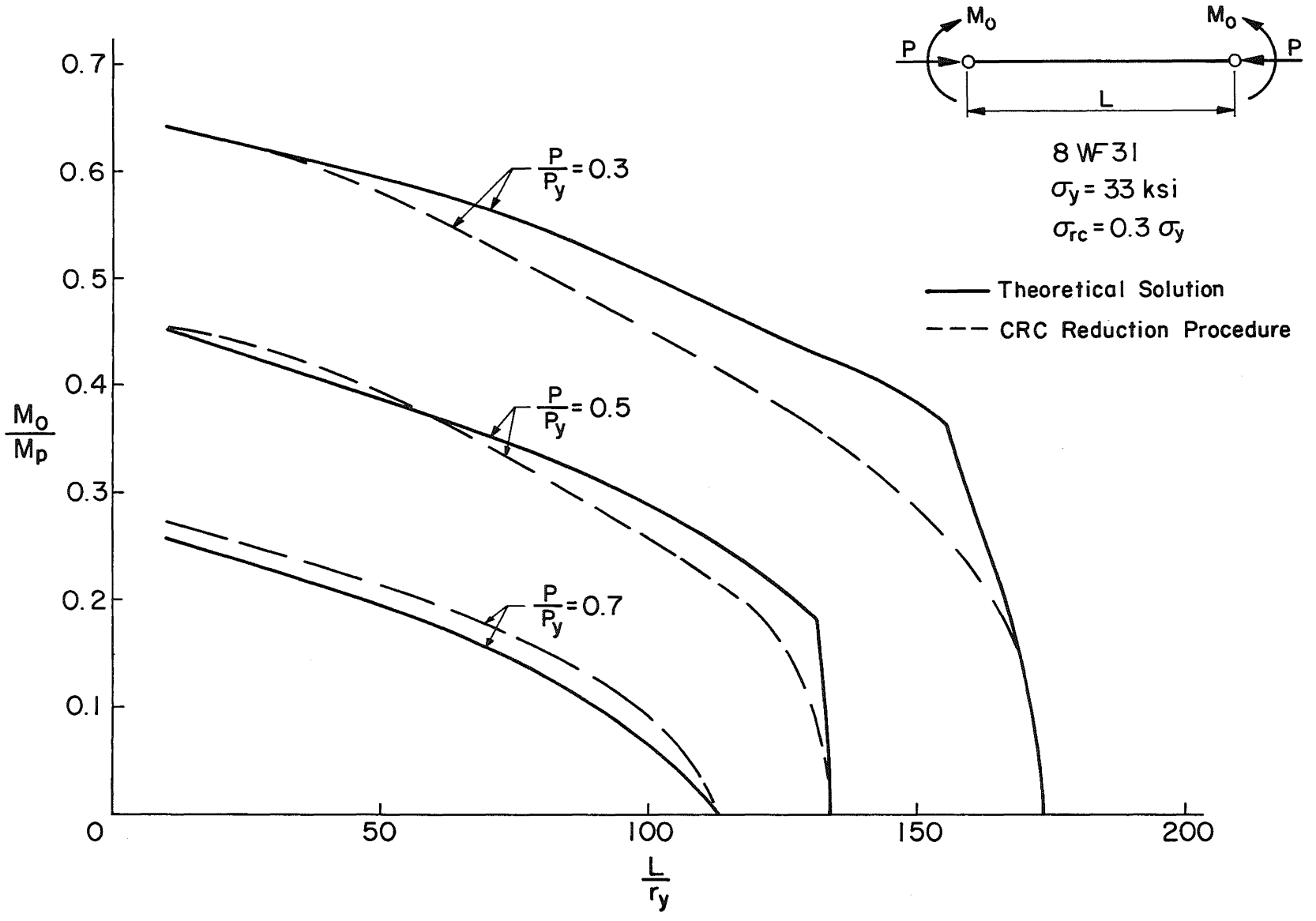

Fig. 14 Comparison with CRC Formula $\rho = +1.0$ 8WF31

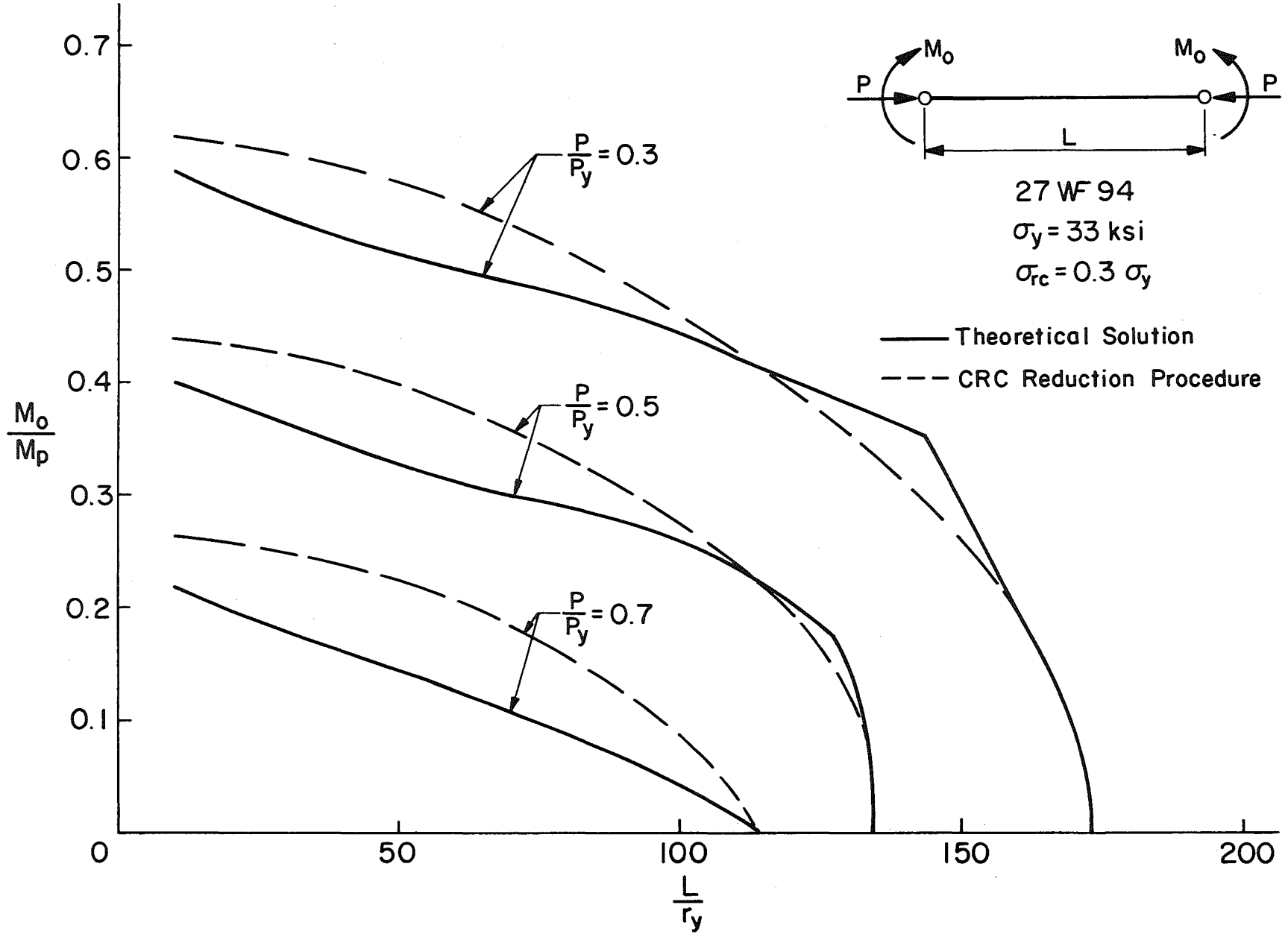

Fig. 15 Comparison with CRC Formula $\rho = +1.0$ 27WF94

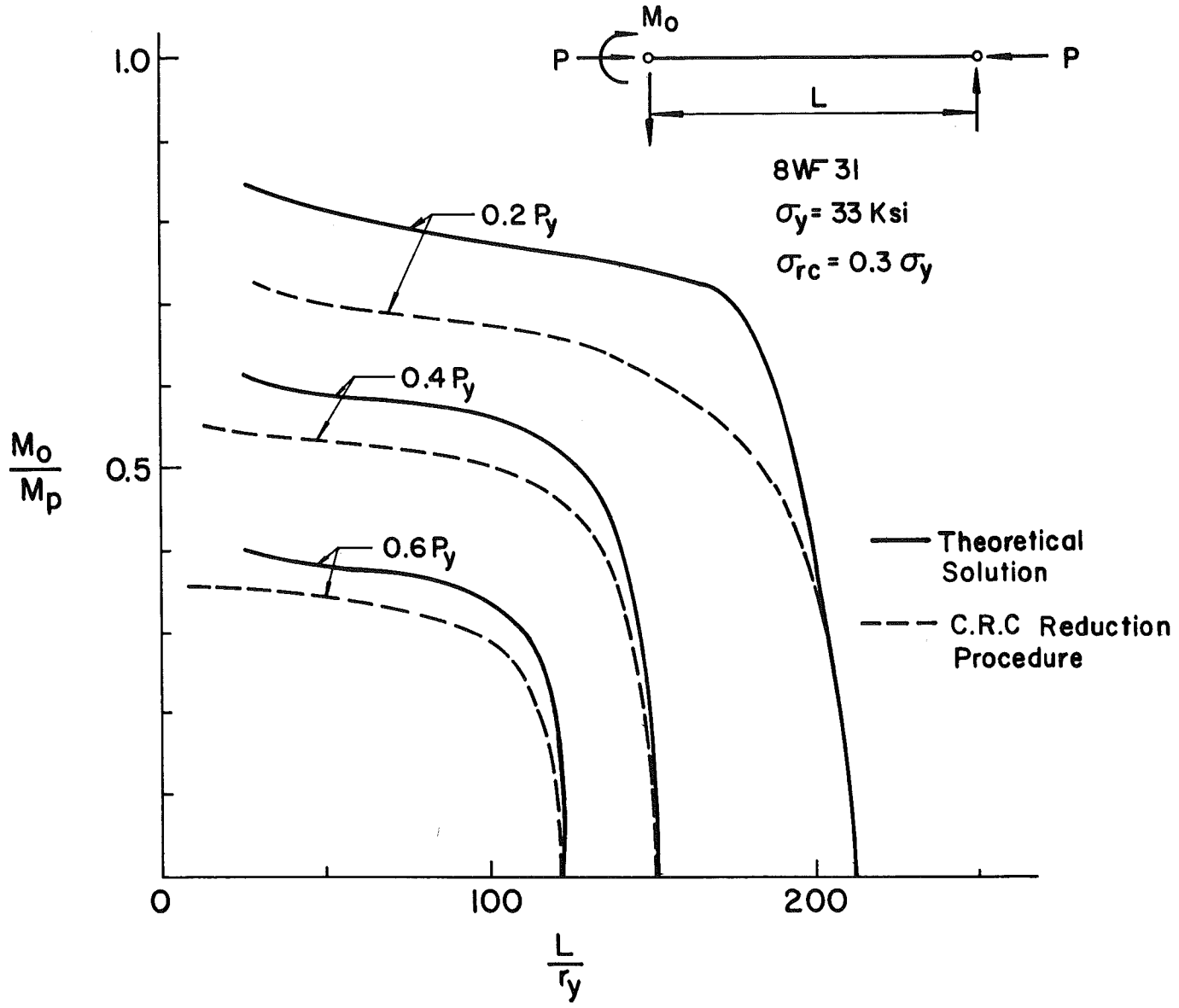

Fig. 16 Comparison with CRC Formula $\rho = 0$ 8WF31

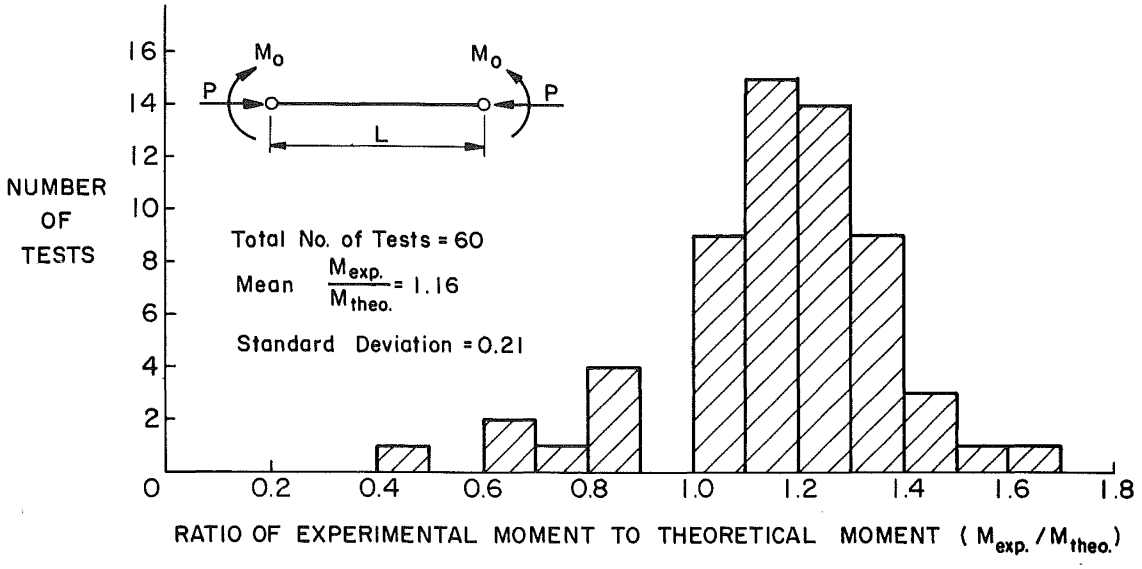

Fig. 17 Frequency Histogram for Test Results $\rho = +1.0$

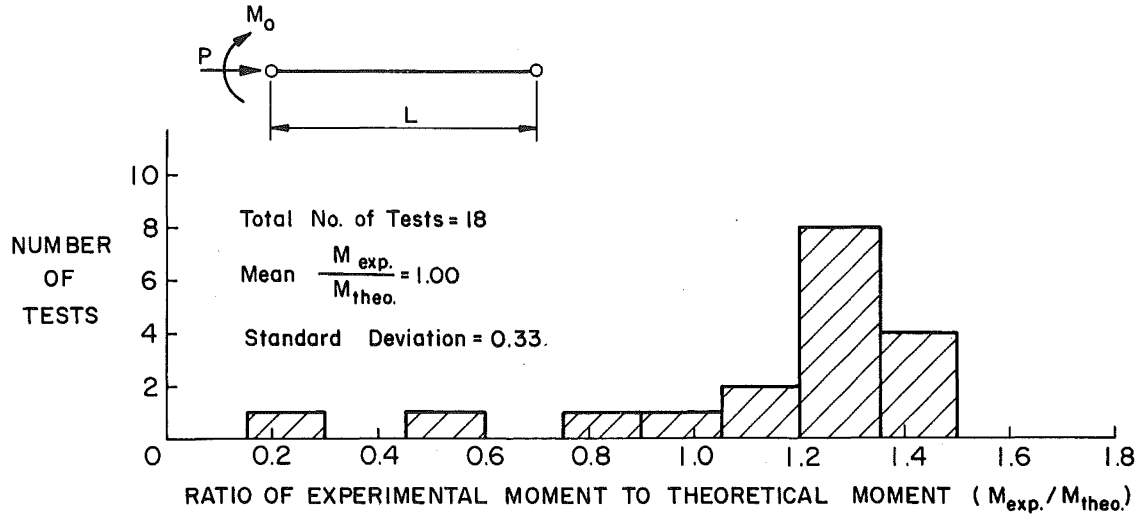

Fig. 18 Frequency Histogram for Test Results $\rho = 0$

REFERENCES

1. Galambos, T. V.
INELASTIC LATERAL-TORSIONAL BUCKLING OF ECCENTRICALLY LOADED WIDE-FLANGE COLUMNS
Ph.D. Dissertation, Lehigh University, June 1959

2. Fukumoto, Y.
INELASTIC LATERAL-TORSIONAL BUCKLING OF BEAM-COLUMNS
Ph.D. Dissertation, Lehigh University, October 1963

3. Galambos, T. V.
INELASTIC LATERAL BUCKLING OF BEAMS
Proc. ASCE, Vol. 89, ST 5, October 1963

4. Galambos, T. V.; Fukumoto, F.
INELASTIC LATERAL-TORSIONAL BUCKLING OF BEAM-COLUMNS
Fritz Laboratory Report No. 205A.34, August 1963

5. Timenshenko, S. P.; Gere, J. M.
THEORY OF ELASTIC STABILITY
McGraw-Hill Book Company, Inc., New York, 1961

6. Bleich, F.
BUCKLING STRENGTH OF METAL STRUCTURES
McGraw-Hill Book Company, Inc., New York, 1952

7. Lay, M. G. and Gimsing, N.
FURTHER STUDIES OF THE MOMENT-THRUST-CURVATURE RELATIONSHIP
Fritz Laboratory Report No. 297.4, January 1964

8. Aglietti, R. A., Lay, M. G. and Galambos, T. V.
TESTS ON A-36 and A441 STEEL BEAM COLUMNS
Fritz Laboratory Report No. 278.14, June 1964

9. Ojalvo, M.
RESTRAINED COLUMNS
Proc. ASCE, Vol. 86, EM5, October 1960

10. Salvadori, M.
LATERAL BUCKLING OF I BEAMS
Trans. ASCE, Vol. 120, p. 1028, 1955

11. Salvadori, M.
LATERAL BUCKLING OF ECCENTRICALLY LOADED I COLUMNS
Trans. ASCE, Vol. 121, p. 1163, 1956

12. Lay, M. G. and Galambos, T. V.
END-MOMENT-END-ROTATION CHARACTERISTICS OF BEAM-COLUMNS
Fritz Laboratory Report No. 205A.35, May 1962

13. Galambos, T. V. and Ketter, R. L.
COLUMNS UNDER COMBINED BENDING AND THRUST
Proc. ASCE, EM2, April, 1959

14. Baker, J. F., Horne, M. R. and Heyman, J.
THE STEEL SKELETON
Vol. 2, University Press, Cambridge, 1956

15. AISC
STEEL CONSTRUCTION MANUAL
American Institute of Steel Construction
Sixth Edition, 1963

16. Ketter, R. L., Beedle, L. S. and Johnston, B. G.
PLASTIC DEFORMATION OF WIDE-FLANGE BEAM COLUMNS
Trans. ASCE, Vol. 120, p. 1028, 1955

17. Adams, P. F., Lay, M. G. and Galambos, T. V.
EXPERIMENTS ON HIGH STRENGTH STEEL MEMBERS
Fritz Laboratory Report No. 297.8, July 1964

18. Column Research Council
GUIDE TO DESIGN CRITERIA FOR METAL COMPRESSION MEMBERS
CRC, Ann Arbor, Michigan, 1960

19. Massonnet, C. and Campus, F.
RECHERCHES SUR LE FLAMBENTENT DE COLONNES EN ACIER A37, A PROFIL EN DOUBLE TE, SOLLICITEES OBLIQUEMENT
I.R.S.I.A. Bulletin No. 17, April 1956

20. SECOND PROGRESS REPORT OF THE SPECIAL COMMITTEE ON STEEL COLUMNS
Paper No. 1789, Trans. ASCE, Vol. 95, 1931

21. Johnston, B. G. and Cheney, L.
STEEL COLUMNS OF ROLLED WIDE FLANGE SECTION
Progress Report No. 2, American Institute of Steel Construction, November 1942

22. Ketter, R. L., Beedle, L. S. and Johnston, B. G.
COLUMN STRENGTH UNDER COMBINED BENDING AND THRUST
The Welding Journal 31(12), Research Supplement 607-S to 662-S, 1952

23. Beedle, L. S. Ready, J. A. and Johnston, B. G.
TESTS OF COLUMNS UNDER COMBINED THRUST AND MOMENT
Proc. SESA, Vol. VIII, No. 1, 109, 1950